Medicinal Chemistry

International Edition: DOI: 10.1002/anie.201610957
German Edition: DOI: 10.1002/ange.201610957

A PDE6δ-KRas Inhibitor Chemotype with up to Seven H-Bonds and Picomolar Affinity that Prevents Efficient Inhibitor Release by Arl2

Pablo Martín-Gago[+], Eyad K. Fansa[+], Christian H. Klein[+], Sandip Murarka[+], Petra Janning, Marc Schürmann, Malte Metz , Shehab Ismail, Carsten Schultz-Fademrecht, Matthias Baumann, Philippe I. H. Bastiaens, Alfred Wittinghofer,* and Herbert Waldmann**

Abstract: *Small-molecule inhibition of the interaction between the KRas oncoprotein and the chaperone PDE6δ impairs KRas spatial organization and signaling in cells. However, despite potent binding in vitro ($K_D < 10$ nM), interference with Ras signaling and growth inhibition require 5–20 μM compound concentrations. We demonstrate that these findings can be explained by fast release of high-affinity inhibitors from PDE6δ by the release factor Arl2. This limitation is overcome by novel highly selective inhibitors that bind to PDE6δ with up to 7 hydrogen bonds, resulting in picomolar affinity. Their release by Arl2 is greatly decreased, and representative compounds selectively inhibit growth of KRas mutated and -dependent cells with the highest activity recorded yet. Our findings indicate that very potent inhibitors of the KRas-PDE6δ interaction may impair the growth of tumors driven by oncogenic KRas.*

Ras proteins are mutated in about 20–30% of human cancers, with the KRas isoform most frequently mutated.[1–4] However, direct targeting of KRas[4–10] by small molecules has not yet given rise to clinical candidates.[11–22]

KRas signaling and spatial organization critically depend on recognition of its farnesylated C-terminal cysteine methyl ester.[23–26] Small-molecule inhibition of the KRas-PDE6δ interaction impairs KRas localization and oncogenic signaling and blocks proliferation of human pancreatic ductal adenocarcinoma (hPDAC) cells harboring oncogenic KRas.[27,28]

The KRas-PDE6δ inhibitors Deltarasin (**1**) and Deltazinone 1 (**2**) bind PDE6δ with low nanomolar affinity in vitro (Figure 1A, B; Deltazinone 1: $K_D = 8 \pm 4$ nM), but show cellular activity only at micromolar concentrations (for example, 5–20 μM Deltazinone 1).[28]

The release factor Arl2 stabilizes PDE6δ and causes a discharge of the medium affinity KRas cargo ($K_D =$ 453 nM).[26] We now demonstrate that Arl2 also induces release of the high affinity inhibitors Deltarasin and Deltazinone 1, which explains why micromolar concentrations are required to effectively reduce cell growth. We describe a novel PDE6δ inhibitor chemotype with picomolar affinity, which prevents efficient release by Arl2.

Release of high-affinity cargo from PDE6δ by Arl2 was analyzed by means of fluorescence polarization measurements. These experiments revealed that in the presence of 200-fold excess of unlabeled compound to prevent re-binding, fluorescently labeled inhibitors **1L*** and **2L*** (Figure 1A,B) are rapidly released by Arl 2 with $k_{off} = 38 \pm 1$ and $19 \pm 1\ s^{-1}\,10^{-3}$, respectively (Figure 2C). These results and the fact that the concentration of Arl2 is also in the micromolar range (Wittinghofer et al., unpublished results) explains why ligand concentrations much higher than expected from the determined K_D values are needed to consistently establish PDE6δ inhibition in cells and to reduce cell growth.

Screening of our in-house compound library (ca. 200000 compounds) employing the Alfa Screen technology[27] for compounds with higher potency identified bis-sulfonamides (for example **3**; $K_D = 13 \pm 4$ nM; Figure 1C) as novel potent ligands of the prenyl binding pocket of PDE6δ.

By analogy to Deltazinone 1,[28] compound **3** displays three H-bonds to R61, Q78, and Y149 (Figure 3A) and two additional interactions with the aromatic rings of W32 and W90. An additional piperidin-4-ylmethyl H-bond donor (for syntheses, see the Supporting Information) occupied more space and formed a new H-bond with the carbonyl group of C56 to yield ligand **4** ($K_D = 8 \pm 2$ nM, Figure 1C and 3B). Binding is further enhanced by a sulfur–π interaction to M117.

To establish an additional H-bond interaction with the E88 side-chain, which plays a major role in KRas binding to PDE6δ,[29] a (2-(methylamino)pyrimidin-4-yl)methyl substituent was introduced to give inhibitor **5** (Deltasonamide 1, Figure 1C). Deltasonamide 1 displays two new water-mediated H-bonds to the aromatic pyrimidine nitrogen atoms

[*] C. H. Klein,[+] Prof. Dr. P. I. H. Bastiaens
Department of Systemic Cell Biology
Max Planck Institute of Molecular Physiology
44227 Dortmund (Germany)
E-mail: philippe.bastiaens@mpi-dortmund.mpg.de
Dr. P. Martín-Gago,[+] Dr. S. Murarka,[+] Dr. P. Janning, Dr. M. Schürmann, M. Metz , Prof. Dr. H. Waldmann
Department of Chemical Biology
Max Planck Institute of Molecular Physiology
44227 Dortmund (Germany)
E-mail: herbert.waldmann@mpi-dortmund.mpg.de
Dr. E. K. Fansa,[+] Dr. S. Ismail, Prof. Dr. A. Wittinghofer
Structural Biology Group
Max Planck Institute for Molecular Physiology
44227 Dortmund (Germany)
E-mail: alfred.wittinghofer@mpi-dortmund.mpg.de
Prof. Dr. P. I. H. Bastiaens, Prof. Dr. H. Waldmann
TU Dortmund, Faculty of Chemistry and Chemical Biology
44227 Dortmund (Germany)
Dr. C. Schultz-Fademrecht, Dr. M. Baumann
Lead Discovery Center GmbH
44227 Dortmund (Germany)
[+] These authors contributed equally to this work.

Supporting information for this article can be found under: http://dx.doi.org/10.1002/anie.201610957.

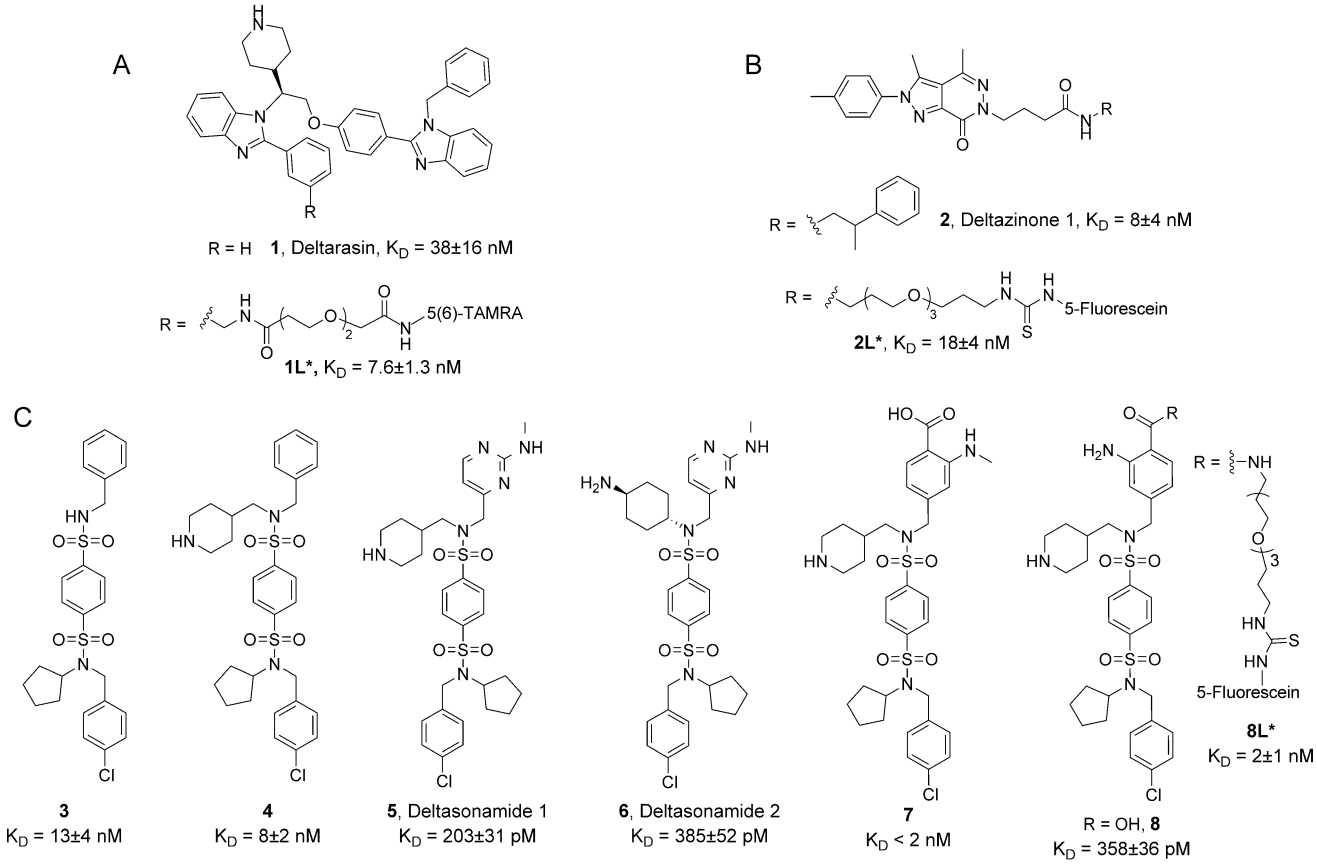

Figure 1. Chemical structures and binding affinities (K_D, determined by competitive fluorescence polarization assay of three independent experiments, see the Supporting Information for details) of Deltarasin and labeled Deltarasin (A, **1** and **1L***), Deltazinone 1 and labeled Deltazinone 1 (B, **2** and **2L***), the newly developed bis-sulfonamides (C, **3**–**8**), and a fluorescently labeled bis-sulfonamide derivative (C, **8L***). For kinetic solubility and schematic binding modes, see the Supporting Information, Figure S1.

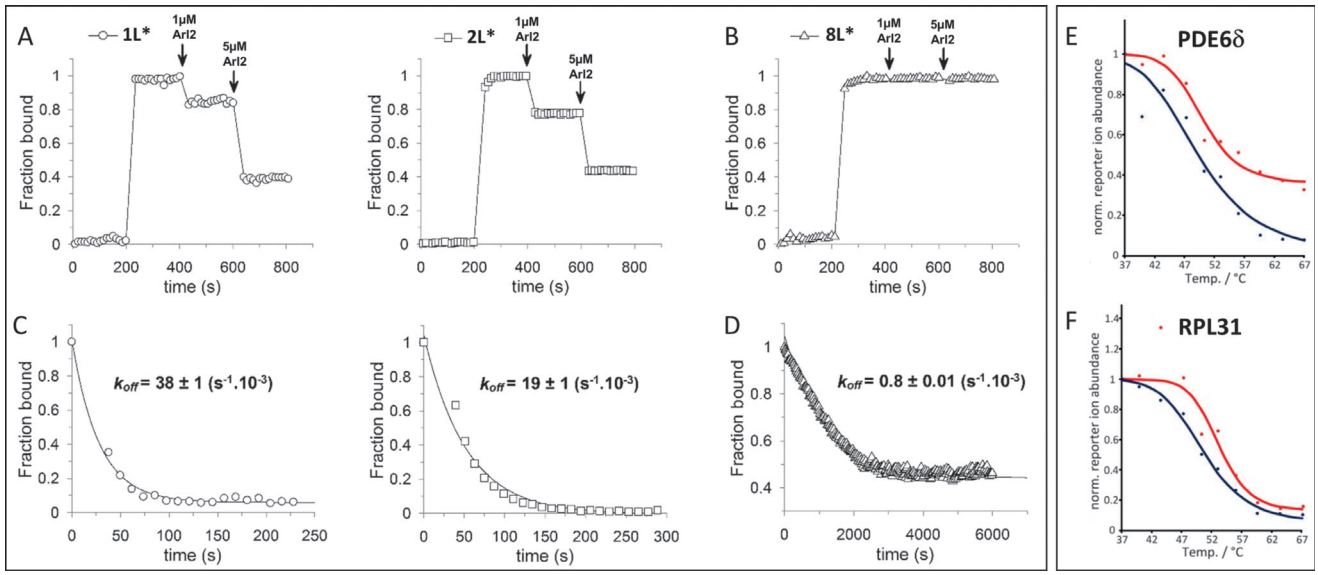

Figure 2. Arl2-mediated displacement of the different chemotypes and CETSA melting curves. A),B) Release by Arl2 under equilibrium conditions of **1L***, **2L***, and **8L***. 0.2 μM fluorescently labeled inhibitor was placed in a cuvette, followed by the addition of 0.5 μM PDE6δ resulting in the increase of the polarization signal owing to complex formation. The formed complex was titrated with Arl2 (1 and 5 μM) as indicated. C),D) Kinetics of release by Arl2 under competition with an unlabeled inhibitor. A mixture of 0.5 μM Arl2 and 40 μM **5** was added to a preformed complex of 0.2 μM of the fluorescently labeled inhibitor and 0.5 μM PDE6δ. The Arl2- mediated release was monitored by the decrease of the polarization. Dissociation rate constants (k_{off}) were obtained by single exponential fitting of the data. E),F) Representative melting curves for PDE6δ (E) and RPL31 (F) as observed in a thermal protein profiling experiment. Melting curves for the DMSO controls are shown in dark blue and melting curves after treatment with inhibitor **8** are shown in red.

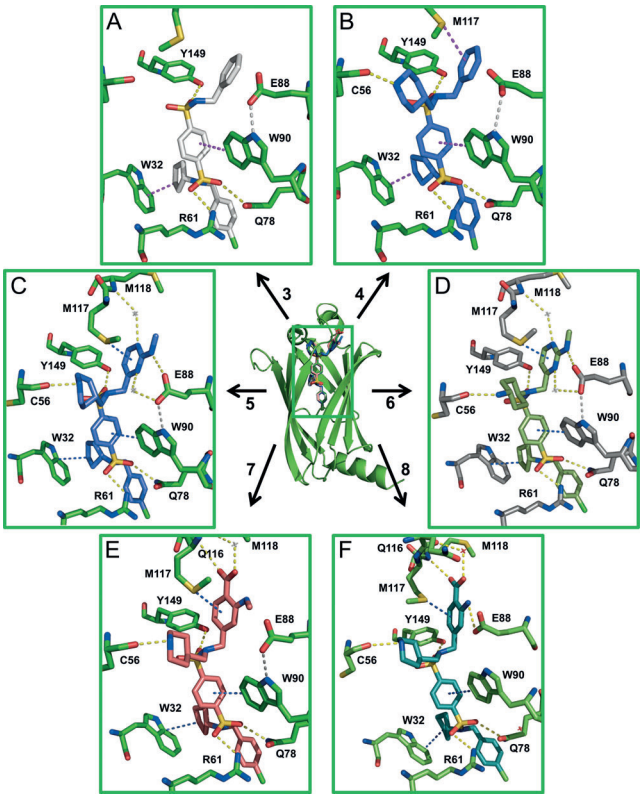

Figure 3. Comparison among the binding modes of inhibitors **3**–**8**. Crystal structure of inhibitor **3** (A; PDB code: 5ML2), **4** (B; PDB: 5ML8), **5** (C, Deltasonamide 1; PDB: 5ML3), **7** (E; PDB: 5ML4), and **8** (F; PDB: 5ML6) in complex with PDE6δ and best docking pose of **6** (D, Deltasonamide 2). Important H-bonding interactions of the ligand to the protein (dotted yellow line) between PDE6δ residues (gray) and aromatic–π interactions (blue) are shown. Only key amino acids are displayed as sticks (see also the Supporting Information).

(Figure 3C). A total of 10 non-covalent interactions stabilize the binding of Deltasonamide 1 inside the PDE6δ binding pocket, including H-bonds to R61, Q78, E88, and Y149 side-chains, to the carbonyl of C56, two water molecule-mediated H-bonds to the Glu88 side-chain and the amide proton of M118, two aromatic–π interactions to the indole side-chains of W32 and W90, and one M117–aryl interaction. This enhanced the in vitro potency to the picomomolar level ($K_D = 203 \pm 31$ pM; see the Supporting Information and Figure S3). The side-chains of E88 and W90 are in an arrangement characteristic for the open RheB-bound conformation of PDE6δ.[26,29] Alternative introduction of a 4-aminocyclohexane moiety resulted in an analogous binding mode, and compound **6** (Deltasonamide 2, Figure 1C) displayed picomolar affinity as well ($K_D = 385 \pm 52$ pM) (Figure 3D).

Energetically favorable replacement of a water molecule with less than three H-bonds[30] by a carboxylate pointing towards M118 yielded compound **7** (Figures 1C and 3E). An additional water molecule establishes a new H-bond between the carboxylate and the carbonyl backbone of Q116. Compound **7** maintains high in vitro potency, but lacks the H-bond to the E88 side-chain, probably because an intramolecular H-bond between the carboxylate and the aniline proton forces the methyl substituent out of the pocket. Removal of the methyl group yielded inhibitor **8** (Figure 1C and 3F), which binds to PDE6δ with a total of 7 H-bonds, including a H-bond with E88, and 3 aromatic–π interactions ($K_D = 358 \pm 36$ pM).

Measurement of apparent permeability (Papp) from the apical (A) to the basolateral (B) side of Caco-2 cells (see the Supporting Information for details) revealed that both Deltasonamide 1 and 2 migrate slowly but show enhanced apparent permeability from the B to A side suggesting a potential interaction with efflux transporters. However, this effect is only moderate.

Assessment of general cytotoxicity employing human peripheral blood mononuclear cells (hPBMCs) revealed that, in contrast to Deltarasin,[28] Deltasonamides 1 and 2 do not impair hPMBC proliferation up to 30 μM concentration.

Labeling of **8** at the carboxylic acid that points towards the exit of the prenyl binding tunnel (Supporting Information, Figure S2) yielded fluorescent analogue **8L*** (Figure 1C). Notably, in contrast to Deltarasin and Deltazinone 1, **8L*** could not be directly displaced from PDE6δ by 5 and even 25 equiv of Arl2 (Figure 2A vs. 2B) Acceleration of release by 2.5 equiv of Arl2 in the presence of 200-fold excess of non-fluorescent inhibitor was 45- and 25-fold slower than the release of **1L*** and **2L*,** respectively (Figure 2C vs. 2D). Thus, increase of the number of inhibitor-PDE6δ interactions leads to a higher stabilization of the complex and higher resistance to displacement by Arl2.

PDE6δ engagement by inhibitor **8** was confirmed by means of a cellular thermal shift assay (CETSA)[31–33] in which the thermal stabilization of the protein of interest upon ligand binding is determined. Mass spectrometric analysis of Jurkat cell lysate treated with 1 μM compound **8** identified proteins showing a characteristic shift in melting temperature by at least 2 °C, or for which the differences in the signal intensities for at least two characteristic peptides were at least 10% (see the Supporting Information and Figure 2E,F) Ligand **8** only engaged PDE6δ and ribosomal protein L31 (RPL31). Literature analysis did not reveal a link between RPL31, Ras proteins or PDE6δ. Thus, compound **8** is a very selective inhibitor of PDE6δ.

Disruption of the interaction between mCherry-PDE6δ and farnesylated Ras proteins (mCitrine-RheB) in living cells was measured in MDCK cells by FLIM-FRET.[27] The homogenous fluorescence patterns of both proteins in the absence of inhibitor indicate solubilization of mCitrine-RheB by mCherry-PDE6δ (Figure 4A,B), which was also reflected in the high molar fraction α of interacting mCitrine-RheB and mCherry-PDE6δ as derived from global analysis of FLIM data.[34] Treatment with increasing concentrations of Deltasonamides resulted in a reduced interacting fraction α of RheB-PDE6δ. Fitting the dose-dependent measurements to an equilibrium model with a clamped compound concentration[27] yielded an apparent "in-cell" K_D of 85 ± 18 nM for Deltasonamide 1 and 61 ± 5 nM for Deltasonamide 2. In contrast to Deltarasin,[27] these apparent K_D values surpass the in vitro measured K_D values by an order of magnitude. If the partitioning coefficient P of the compounds between cytoplasm and extracellular environment is independent of administered compound concentration, the ratio of the in vivo and in vitro K_D values reflect P. This indicates that

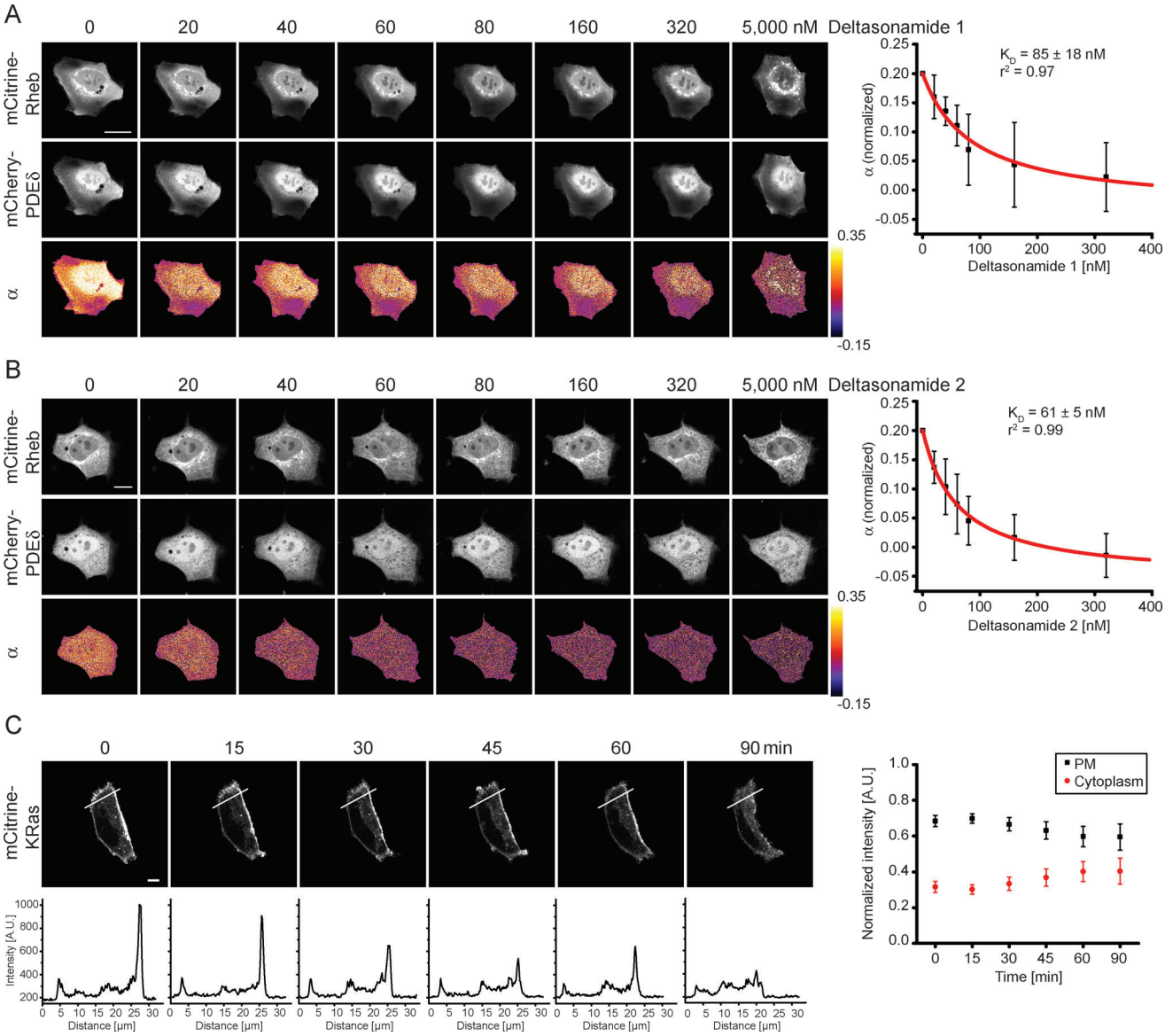

Figure 4. Inhibition of the interaction between Ras proteins and PDE6δ in cells by Deltasonamides resulting in delocalization. A),B) Left: FLIM measurements of the mCitrine-RheB and mCherry-PDE6δ interaction in dependence on Deltasonamide dose. Upper and middle rows: fluorescence intensity of mCitrine-RheB and mCherry-PDE6δ. Lower rows: molar fraction α of interacting mCitrine-RheB and mCherry-PDE6δ. Inhibitor concentrations are indicated above each image in nM. Right: fit of averaged dose-response of five cells to a binding model (see methods) yielded an "in-cell" K_D of 85 ± 18 nM (s.e.m.) for Deltasonamide 1 and 61 ± 5 nM for Deltasonamide 2. C) Time series of mCitrine-KRas redistribution upon administration of 5 μM Deltasonamide 2 in MiaPaCa-2. Upper row: fluorescence intensity of mCitrine-KRas, lower row: intensity profiles of corresponding ROI in the images. Right: KRas mean intensity ± s.d. at the plasma membrane (black) and inside the cell (red) over time ($N = 8$).

only about 0.2–0.6% of the extracellular Deltasonamide concentration is available in the cytoplasm to inhibit PDE6δ. In general, this finding is consistent with the Caco-2 permeability data described above and calculated log P/log D values (see the Supporting Information for details). However, in contrast to these data, the apparent K_D values monitor target engagement in cells, as opposed to general membrane permeability.

The new inhibitors also led to a loss of KRas plasma membrane (PM) localization as apparent from MiaPaCa-2 cells ectopically expressing mCitrine-KRas treated with 5 μM Deltasonamide 2 (Figure 4C). Analysis of variance showed significance for loss of PM localization between 0 min and 30 min onwards in agreement with the effective rate of KRas PM dissociation.[24]

Analysis of anti-proliferative activity by means of impedance-based real-time cell analyzer (RTCA) measurements revealed that treatment of the oncogenic KRas-dependent Panc-Tu-I, and MiaPaCa-2[17,18] cells with either Deltasonamide 1 or 2 resulted in a strongly reduced proliferation, even at submicromolar concentrations (Figure 5). This was most pronounced in MiaPaCa-2 cells treated with Deltasonamide 2, with about 50% reduction of growth rate at 750 nM (Figure 5B). Growth of Panc Tu-I cells was reduced by ca.

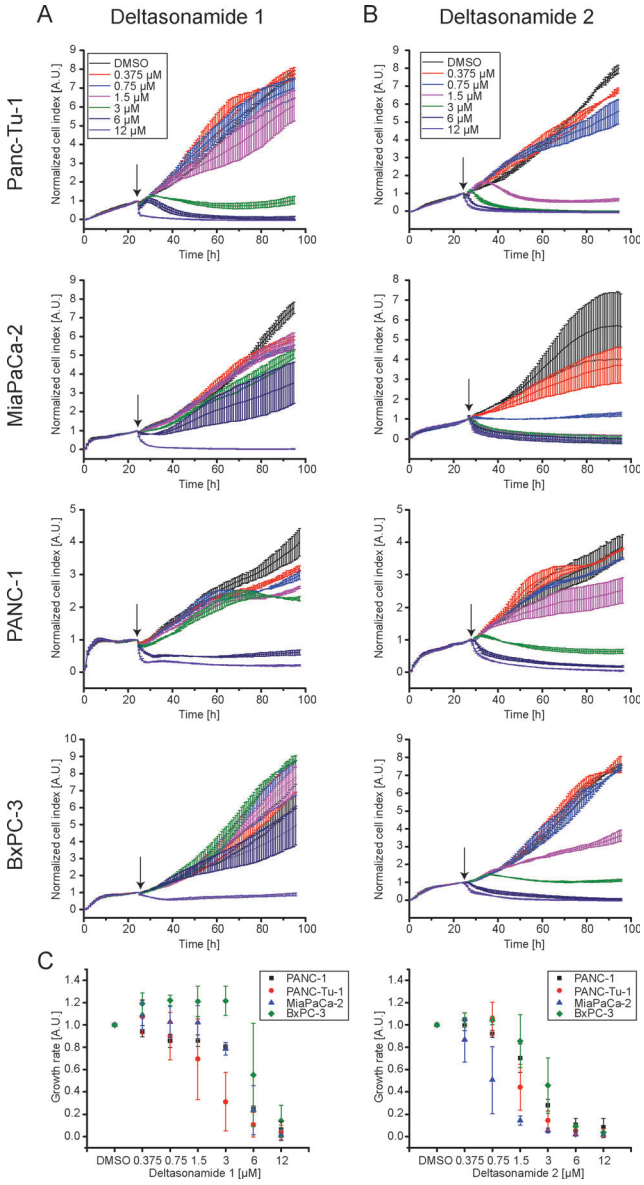

Figure 5. Inhibition of proliferation of human pancreatic cancer cell lines by Deltasonamides. A),B) RTCA of hPDAC cell lines with distinct KRas dependency treated with different doses of Deltasonamide 1 (left column) or Deltasonamide 2 (right column). Cell indices ± s.d. were measured in duplicates and normalized to the time point of drug administration. C) Growth rate ± s.d. in dependence of Deltasonamide dose. The growth rates were estimated by area under the curve integration over 60 h after drug administration and normalized to DMSO control.

50% at 1.5 µM. Thus the compounds are ca. 30-fold more potent than Deltazinone 1. The discrepancy between the concentration of compounds that induce a growth inhibitory effect and their K_D values for PDE6δ is most likely due to their low partitioning coefficient P (ca. 0.2% for Deltasonamide 1 and ca. 0.6% for Deltasonamide 2). This indicates that further compound development should not only concentrate on compound potency, but also on increasing the fraction of compounds available in the cytosol for binding. Both compounds had less activity on the KRas-independent Panc-1 cells and their weakest anti-proliferative effect on KRas wild type BxPC-3 cells.

In conclusion, release of even high-affinity inhibitors by Arl2 activity explains why high inhibitor concentrations are needed to effectively reduce cell growth by PDE6δ inhibition. Highly potent selective inhibitors with up to seven H-bonds and picomolar affinity reduce release by Arl2 and show the highest activity recorded yet in proliferation assays employing KRas mutated and -dependent cell lines. These results suggest that very potent inhibitors of the KRas- PDE6δ interaction may become accessible that impair the growth of tumors driven by oncogenic KRas.

Acknowledgements

This research was supported by the Deutsche Forschungsgemeinschaft (Sonderforschungsbereich SFB 642 to A.W., H.W., and P.I.H.B.), the Deutsche Krebshilfe (Grant 110995 to P.I.H.B.), and the European Research Council under the European Union's Seventh Framework Program (FP7/2007–2013; ERC Grant 322637 to P.I.H.B., ERC Grant 268309 to H.W. and ERC Grant 268782 to A.W.). We are grateful to Andreas Brockmeyer for assistance in the cellular thermal shift assay.

Conflict of interest

The authors declare no conflict of interest.

Keywords: drug design · medicinal chemistry · PDEδ · Ras protein · structure–activity relationships

[1] A. Wittinghofer, *Biol. Chem.* **1998**, *379*, 933–937.
[2] A. E. Karnoub, R. A. Weinberg, *Nat. Rev. Mol. Cell Biol.* **2008**, *9*, 517–531.
[3] Y. Pylayeva-Gupta, E. Grabocka, D. Bar-Sagi, *Nat. Rev. Cancer* **2011**, *11*, 761–774.
[4] A. D. Cox, S. W. Fesik, A. C. Kimmelman, J. Luo, C. J. Der, *Nat. Rev. Drug Discovery* **2014**, *13*, 828–851.
[5] A. Young, J. Lyons, A. L. Miller, V. T. Phan, I. R. Alarcón, F. McCormick, *Adv. Cancer Res.* **2009**, *102*, 1–17.
[6] W. Wang, G. Fang, J. Rudolph, *Bioorg. Med. Chem. Lett.* **2012**, *22*, 5766–5776.
[7] A. T. Baines, D. Xu, C. J. Der, *Future Med. Chem.* **2011**, *3*, 1787–1808.
[8] A. G. Stephen, D. Esposito, R. K. Bagni, F. McCormick, G. K. Abou-Alfa, L. Schwartz, et al., *Cancer Cell* **2014**, *25*, 272–281.
[9] P. M. Cromm, J. Spiegel, T. N. Grossmann, H. Waldmann, *Angew. Chem. Int. Ed.* **2015**, *54*, 13516–13537; *Angew. Chem.* **2015**, *127*, 13718–13741.
[10] J. Spiegel, P. M. Cromm, G. Zimmermann, T. N. Grossmann, H. Waldmann, *Nat. Chem. Biol.* **2014**, *10*, 613–622.
[11] A. G. Taveras, S. W. Remiszewski, R. J. Doll, D. Cesarz, E. C. Huang, P. Kirschmeier, et al., *Bioorg. Med. Chem.* **1997**, *5*, 125–133.
[12] A. Patgiri, K. K. Yadav, P. S. Arora, D. Bar-Sagi, *Nat. Chem. Biol.* **2011**, *7*, 585–587.

[13] T. Maurer, L. S. Garrenton, A. Oh, K. Pitts, D. J. Anderson, N. J. Skelton, et al., *Proc. Natl. Acad. Sci. USA* **2012**, *109*, 5299 – 5304.
[14] Q. Sun, J. P. Burke, J. Phan, M. C. Burns, E. T. Olejniczak, A. G. Waterson, T. Lee, O. W. Rossanese, S. W. Fesik, *Angew. Chem. Int. Ed.* **2012**, *51*, 6140 – 6143; *Angew. Chem.* **2012**, *124*, 6244 – 6247.
[15] F. Shima, Y. Yoshikawa, M. Ye, M. Araki, S. Matsumoto, J. Liao, L. Hu, et al., *Proc. Natl. Acad. Sci. USA* **2013**, *110*, 8182 – 8187.
[16] H. J. Hocker, K.-J. Cho, C.-Y. K. Chen, N. Rambahal, S. R. Sagineedu, K. Shaari, J. Stanslas, J. F. Hancock, A. A. Gorfe, *Proc. Natl. Acad. Sci. USA* **2013**, *110*, 10201 – 10206.
[17] S. M. Lim, K. D. Westover, S. B. Ficarro, R. A. Harrison, H. G. Choi, M. E. Pacold, et al., *Angew. Chem. Int. Ed.* **2014**, *53*, 199 – 204; *Angew. Chem.* **2014**, *126*, 203 – 208.
[18] E. S. Leshchiner, A. Parkhitko, G. H. Bird, J. Luccarelli, J. A. Bellairs, S. Escudero, K. Opoku-Nsiah, M. Godes, N. Perrimon, L. D. Walensky, *Proc. Natl. Acad. Sci. USA* **2015**, *112*, 1761 – 1766.
[19] J. J. G. Winter, M. Anderson, K. Blades, C. Brassington, A. L. Breeze, C. Chresta, et al., *J. Med. Chem.* **2015**, *58*, 2265 – 2274.
[20] M. P. Patricelli, M. R. Janes, L.-S. Li, R. Hansen, U. Peters, L. V. Kessler, Y. Chen, et al., *Cancer Discov.* **2016**, *6*, 316 – 329.
[21] J. M. Ostrem, U. Peters, M. L. Sos, J. A. Wells, K. M. Shokat, *Nature* **2013**, *503*, 548 – 551.
[22] J. M. L. Ostrem, K. M. Shokat, *Nat. Rev. Drug Discov.* **2016**, DOI: 10.1038/nrd.2016.139.
[23] J. F. Hancock, H. Paterson, C. J. Marshall, *Cell* **1990**, *63*, 133 – 139.
[24] M. Schmick, N. Vartak, B. Papke, M. Kovacevic, D. C. Truxius, L. Rossmannek, P. I. H. Bastiaens, *Cell* **2014**, *157*, 459 – 471.
[25] A. Chandra, H. E. Grecco, V. Pisupati, D. Perera, L. Cassidy, F. Skoulidis, S. A. Ismail, et al., *Nat. Cell Biol.* **2012**, *14*, 148 – 158.
[26] S. A. Ismail, Y.-X. Chen, A. Rusinova, A. Chandra, M. Bierbaum, L. Gremer, G. Triola, H. Waldmann, P. I. H. Bastiaens, A. Wittinghofer, *Nat. Chem. Biol.* **2011**, *7*, 942 – 949.
[27] G. Zimmermann, B. Papke, S. Ismail, N. Vartak, A. Chandra, M. Hoffmann, S. A. Hahn, G. Triola, A. Wittinghofer, P. I. H. Bastiaens, et al., *Nature* **2013**, *497*, 638 – 642.
[28] B. Papke, S. Murarka, H. A. Vogel, P. Martín-Gago, M. Kovacevic, D. C. Truxius, E. K. Fansa, et al., *Nat. Commun.* **2016**, *7*, 11360.
[29] S. Dharmaiah, L. Bindu, T. H. Tran, W. K. Gillette, P. H. Frank, R. Ghirlando, D. V Nissley, D. Esposito, F. Mccormick, A. G. Stephen, et al., **n.d.**, DOI: 10.1073/pnas.1615316113.
[30] E. Persch, O. Dumele, F. Diederich, *Angew. Chem. Int. Ed.* **2015**, *54*, 3290 – 3327; *Angew. Chem.* **2015**, *127*, 3341 – 3382.
[31] H. Franken, T. Mathieson, D. Childs, G. M. A. Sweetman, T. Werner, I. Tögel, C. Doce, et al., *Nat. Protoc.* **2015**, *10*, 1567 – 1593.
[32] F. B. M. Reinhard, D. Eberhard, T. Werner, H. Franken, D. Childs, C. Doce, M. F. Savitski, et al., *Nat. Methods* **2015**, *12*, 1129 – 1131.
[33] M. M. Savitski, F. B. M. Reinhard, H. Franken, T. Werner, M. F. Savitski, D. Eberhard, D. Martinez Molina, R. Jafari, R. B. Dovega, S. Klaeger, et al., *Science* **2014**, *346*, 1255784.
[34] H. E. Grecco, P. Roda-Navarro, A. Girod, J. Hou, T. Frahm, D. C. Truxius, R. Pepperkok, A. Squire, P. I. H. Bastiaens, *Nat. Methods* **2010**, *7*, 467 – 472.

Manuscript received: November 14, 2016
Final Article published: ■■ ■■, ■■■■

Communications

Medicinal Chemistry

P. Martín-Gago, E. K. Fansa, C. H. Klein, S. Murarka, P. Janning, M. Schürmann, M. Metz , S. Ismail, C. Schultz-Fademrecht, M. Baumann, P. I. H. Bastiaens,* A. Wittinghofer,* H. Waldmann* _____ ■■■–■■■

A PDE6δ-KRas Inhibitor Chemotype with up to Seven H-Bonds and Picomolar Affinity that Prevents Efficient Inhibitor Release by Arl2

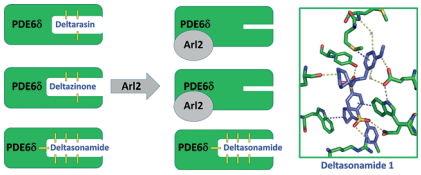

Small-molecule inhibition of the interaction between KRas oncoprotein and the chaperone PDE6δ impairs KRas spatial organization and signaling in cells. Deltasonamides are highly selective inhibitors that bind to PDE6δ with up to 7 hydrogen bonds, resulting in picomolar affinity.